GENETICS

Inheritance of repressed chromatin domains during S phase requires the histone chaperone NPM1

Thelma M. Escobar[1,2]†, Jia-Ray Yu[1,2]‡, Sanxiong Liu[1,2], Kimberly Lucero[1,2], Nikita Vasilyev[1,2]§, Evgeny Nudler[1,2], Danny Reinberg[1,2]*

The epigenetic process safeguards cell identity during cell division through the inheritance of appropriate gene expression profiles. We demonstrated previously that parental nucleosomes are inherited by the same chromatin domains during DNA replication only in the case of repressed chromatin. We now show that this specificity is conveyed by NPM1, a histone H3/H4 chaperone. Proteomic analyses of late S-phase chromatin revealed NPM1 in association with both H3K27me3, an integral component of facultative heterochromatin, and MCM2, an integral component of the DNA replication machinery; moreover, NPM1 interacts directly with PRC2 and with MCM2. Given that NPM1 is essential, the inheritance of repressed chromatin domains was examined anew using mESCs expressing an auxin-degradable version of endogenous NPM1. Upon NPM1 degradation, cells accumulated in the G_1-S phase of the cell cycle and parental nucleosome inheritance from repressed chromatin domains was markedly compromised. NPM1 chaperone activity may contribute to the integrity of this process as appropriate inheritance required the NPM1 acidic patches.

INTRODUCTION

A hallmark of the epigenetic process entails the regulated inheritance of a sufficient platform of gene expression patterns from parental cells such that the original gene expression profile is fully recapitulated in progeny cells, bypassing the reestablishment de novo of a particular cell identity. The structure of chromatin domains can provide such a platform, exhibiting features that either promote chromatin accessibility to the transcription machinery or foster its compaction. Whether or not chromatin domains are heritable was recently resolved (*1*–*3*). A CRISPR-Cas9 biotinylation system revealed the profile of parental nucleosome segregation during DNA replication with single locus specificity: Parental nucleosomes are indeed inherited to the same chromatin domains during S phase but only in the case of repressed and not active chromatin domains (*1*). Transcription activation of a previously repressed locus leads to the dispersal of parental nucleosomes, thereby thwarting inheritance (*1*). This finding points to features inherent to the repressed chromatin state being epigenetic.

Facultative heterochromatin comprises di- and tri-methylated lysine 27 of histone H3 (H3K27me2/me3). The multisubunit polycomb repressive complex 2 (PRC2) contains a subset of the polycomb group of proteins and is the sole enzyme responsible for all states of H3K27 methylation (*4*–*8*). Notably, the EED subunit of PRC2 recognizes the product of PRC2 catalysis, H3K27me3, resulting in an allosteric activation of PRC2 and stimulation of its histone methyltransferase activity conveyed by its EZH2 subunit (*9*). This feed-forward mechanism accounts for the formation of extensive, repressive facultative heterochromatin domains (*4*, *10*). In addition, given that only repressed chromatin domains are inherited, we postulate that this feed-forward mechanism can account for the full restoration of repressive chromatin domains upon DNA replication: H3K27me3 within locally segregated parental nucleosomes provides the allosteric activator that stimulates PRC2 catalysis of the trimethyl modification on newly incorporated naïve nucleosomes (Fig. 1A). Yet, these findings and the ensuing reasoning beg the question as to what process provides specificity such that parental nucleosome inheritance is limited to repressed chromatin domains. To address this aspect of the epigenetic process, we investigated proteins associated with late S-phase replicating, facultative heterochromatin and found that the histone chaperone, nucleophosmin (NPM1), exhibits an integral role in this process.

RESULTS

Replicating repressive chromatin domains are enriched in NPM1

As euchromatic regions are replicated at early times of S phase and heterochromatin is replicated later (*11*), we compared a proteomic analysis of chromatin containing H3K27me2/me3 at early and late times of S phase. Mouse embryonic stem cells (mESCs) expressing endogenous, FLAG–biotin acceptor protein (BAP)–tagged versions of four H3.1 alleles (fig. S1A) (*3*) were infected with lentivirus expressing a hemagglutinin (HA)–tagged version of minichromosome maintenance protein 2 (MCM2) (fig. S1D), an integral component of the DNA replication machinery that makes the first contact with parental nucleosomes (*12*, *13*). After synchronization at the G_1-S boundary using a double thymidine block, the cells were released into S phase for 2 or 6 hours (early or late S phase, respectively; fig. S1B). Chromatin specific to early or late S phase was isolated and cross-linked, and 200– to 500–base pair (bp) fragments were subjected first to FLAG-H3.1 immunoprecipitation (IP) with the resulting eluate being halved and subjected to IP against either H3K27me2/me3 or HA-MCM2 (Fig. 1B). Mass spectrometric analyses identified specific proteins associated with both H3.1 and H3K27me2/me3 in early versus late S-phase

[1]Department of Biochemistry and Molecular Pharmacology, New York University Grossman School of Medicine, New York, NY, USA. [2]Howard Hughes Medical Institute, New York University Grossman School of Medicine, New York, NY, USA.
*Corresponding author. Email: danny.reinberg@nyumc.org
†Present address: Department of Biochemistry and Institute for Stem Cell and Regenerative Medicine, University of Washington, Seattle, WA 98109, USA.
‡Present address: Fralin Biomedical Research Institute at VTC, Children's National Research & Innovation Campus, Washington, DC 20012, USA.
§Present address: Regeneron Pharmaceuticals Inc., 777 Old Saw Mill River Road Tarrytown, NY 10591, USA.

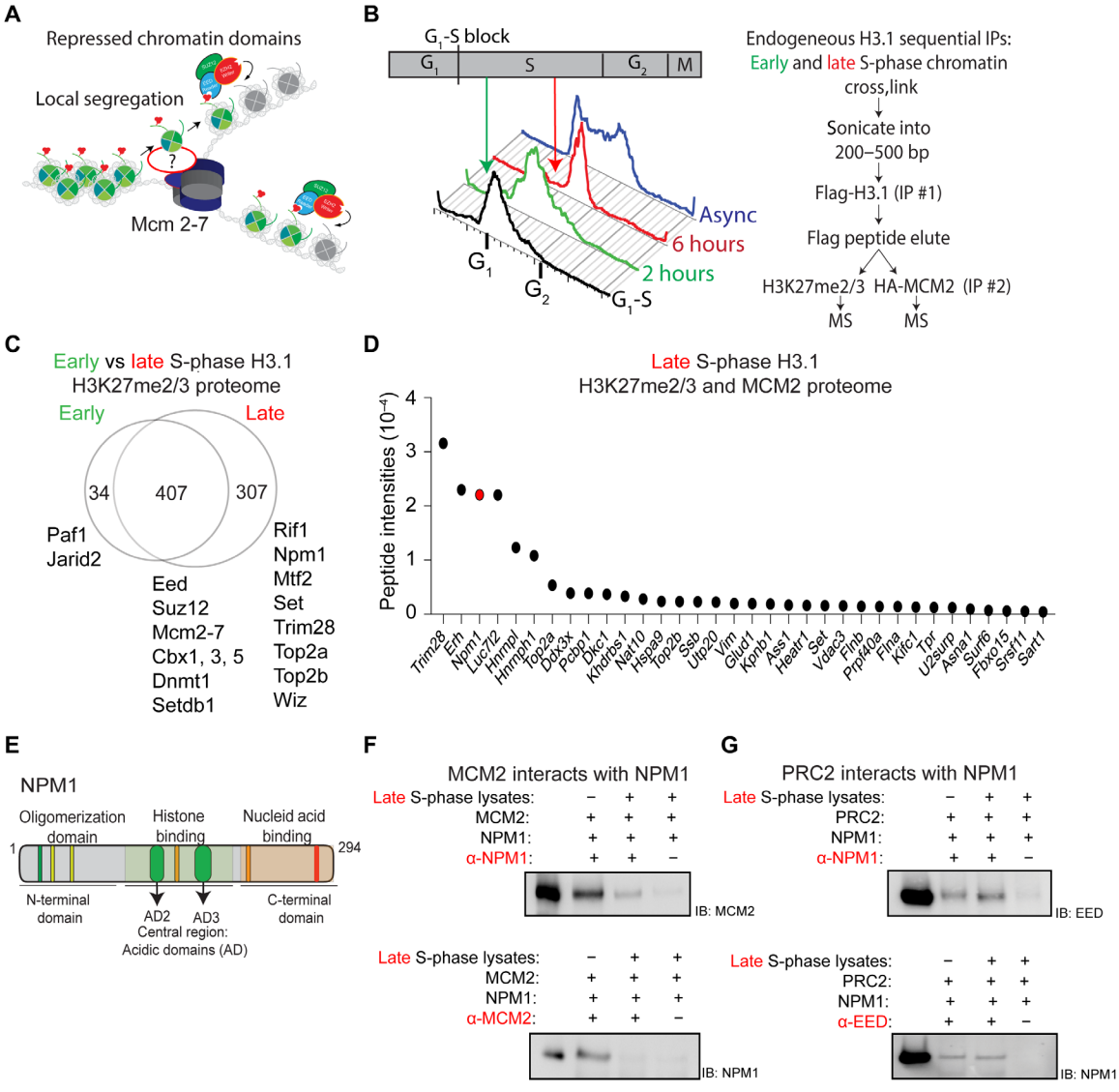

Fig. 1. H3.1-proteome analysis identifies NPM1 in late H3K27me2/3-replicating chromatin domains. (**A**) Schematic illustration of repressed chromatin domains across the DNA replication fork (MCM2-7). Parental nucleosomes (green) segregate randomly to the leading and lagging DNA strands within the same chromatin domain. PRC2 recognizes H3K27me3 (red triplet) within parental nucleosomes resulting in its allosteric activation and propagation of H3K27me3 to naïve nucleosomes (gray). (**B**) Experimental setup for chromatin immunoprecipitations (ChIPs) followed by mass spectrometry in mESCs to identify H3.1-associated proteins in late S phase. mESCs were synchronized at G_1-S and released for either 2 hours (early S phase) or 6 hours (late S phase), and chromatin was isolated for sequential ChIPs that were performed as depicted. (**C**) Unique polypeptides identified from H3.1 and H3K27me2/3 proteome analysis within early and late S phase reproduced from four independent experiments. (**D**) The 307 polypeptides identified in late H3K27me2/3 from (C) were cross-referenced with the late MCM2–replicative proteome (two independent experiments) to identify the H3.1-proteome present in both H3K27me2/me3 and HA-MCM2. Protein intensities were calculated by the sum of peptide intensities extracted from MS1 spectra minus the polypeptides obtained from IPs of untagged-H3.1 control. (**E**) Schematic showing NPM1 protein domains comprising an N-terminal oligomerization domain, its central region containing two acidic domains (AD2 and AD3) that exhibit histone binding and chaperone activities, and its C-terminal domain comprising nucleic acid binding activity. (**F** and **G**) Reciprocal IPs of recombinant NPM1 and either recombinant MCM2 (F) or core PRC2 (G) with and without incubation with late S-phase lysates, as indicated. In each case, the unmarked first lane shows a mixture of 100 ng of each recombinant protein as input.

cells (Fig. 1C and table S1), with no significant variation in canonical H3 between S-phase stages (fig. S1C). PRC2 association was detected in both cases as evidenced by the presence of its EED and SUZ12 subunits, as were components of the DNA replication machinery, MCM2 to MCM7 (Fig. 1C and table S1). Of note, replication timing regulator factor 1 (RIF1), the replication timing regulator that associates with late replicating regions (*14*), was captured in the late S-phase H3.1/H3K27me2/me3 proteome along with the H3/H4 histone chaperone, NPM1 (Fig. 1C). Moreover, NPM1 expression at the protein level is stable throughout the cell cycle with evidence supporting its multiple roles including facilitating DNA replication during S phase (*15*). Notably, our previous proteomic analysis involving PRC2 revealed its association with NPM1 (*10*). Among the proteins identified as being common to both H3.1/H3K37me2/me3 and H3.1/MCM2 proteomes from late S phase, NPM1 was one of the prominent candidates (Fig. 1D).

We next examined whether NPM1 interacts with PRC2 and/or MCM2 using recombinant versions of NPM1 and MCM2 (fig. S1E) and the purified core PRC2. Reciprocal IPs demonstrated that NPM1 interacted directly with MCM2 and that this interaction did not require other proteins present in late S-phase extract, the addition of which appeared instead to be interfering (Fig. 1F). Similarly, reciprocal IPs demonstrated a direct interaction between NPM1 and PRC2, and the addition of late S-phase extract in this case was ineffectual (Fig. 1G). We validated these in vitro direct interactions using pull-downs in late S-phase mESC extract with which we observed a reciprocal interaction between NPM1 and PRC2 as well as between NPM1 and MCM2 (fig. S1, F to H). Thus, NPM1 interacted directly with major activities involved in either DNA replication (MCM2) or facultative heterochromatin formation (PRC2).

Among its many reported biological functions (*16*), NPM1 interaction with histones has implicated this protein in several chromatin-based processes, including DNA replication and repair, transcription, and chromatin remodeling (*12*, *17*). The distinct NPM1 protein domains include a central region with acidic patches (Fig. 1E), which exhibits histone-binding activity with a strong preference for histone H3/H4 tetramers, relative to histone H2A/H2B dimers (*18*). These acidic regions are critical for the histone H3/H4 chaperone activity of NPM1 in vitro (*18*) and in vivo (see below, fig. S4). Given its reported H3/H4 chaperone activity in vitro (*18*, *19*) and our findings here that NPM1 associates with late S-phase chromatin and directly interacts with both MCM2 and PRC2, we investigated the possibility that NPM1 facilitates repressed chromatin domain inheritance.

Inducible degradation of NPM1 alters cell-cycle progression

As NPM1 is required for cell viability (*20*), we used the auxin-inducible degradation (AID) system (*21*, *22*) to deplete cellular NPM1 upon auxin addition. The endogenous NPM1 gene in mESCs having four FLAG-BAP–tagged versions of histone H3.1 used above (fig. S1A) was engineered to express an AID-tag at its N terminus using CRISPR-Cas9 technology (Fig. 2A, left, and see below). AID-NPM1 was undetectable by Western blot at 6 hours of auxin treatment (Fig. 2A, right). To ascertain a time period during which auxin addition would be not only sufficient to deplete AID-NPM1 without affecting cell survival but also tenable for analyzing parental nucleosome inheritance as preformed previously (*1*), we first analyzed cells treated for 24 and 48 hours with auxin. Protracted auxin treatment gave rise to severe defects in cell proliferation evident after 48 hours (Fig. 2B). At 24 hours, the AID-NPM1 cells already exhibited an abnormal blockage at G_1, relative to untreated cells (Fig. 2C). The salient features associated with facultative heterochromatin were gauged as a function of time after auxin addition by Western blot. While AID-NPM1 was undetectable by 6 hours of auxin treatment, auxin treatment for up to 24 hours was ineffectual with respect to the levels of the core PRC2 subunits: SUZ12, EZH2, and EED (fig. S2).

S-phase depletion of NPM1 perturbs gene expression

These above findings suggested that a 12-hour auxin treatment would not only be sufficient for AID-NPM1 depletion but also satisfy the 12-hour time frame previously established for examining parental nucleosome inheritance after release into S phase [(*1*) and see below]. Thus, we next examined the phenotype of these AID-NPM1 cells that were blocked at the G_1-S boundary and then released into S phase for 12 hours, with and without auxin treatment (Fig. 3A, top). As expected, NPM1 was depleted within 6 hours (Fig. 3A, bottom). The cell-cycle profile after release into S phase for 6 hours was similar, without and with auxin treatment (Fig. 3B, top middle and right, respectively), while cells released into S phase for 12 hours showed evidence of a G_1 blockage in the subsequent cell cycle in the case of auxin-treated, relative to untreated cells (Fig. 3B, bottom right and middle, respectively, and Fig. 3C). This perturbation of the cell-cycle profile was accompanied by the occurrence of differentially expressed genes (DEGs), reflective of aberrant up- and down-regulated gene expression (Fig. 3D and table S2). Notably,

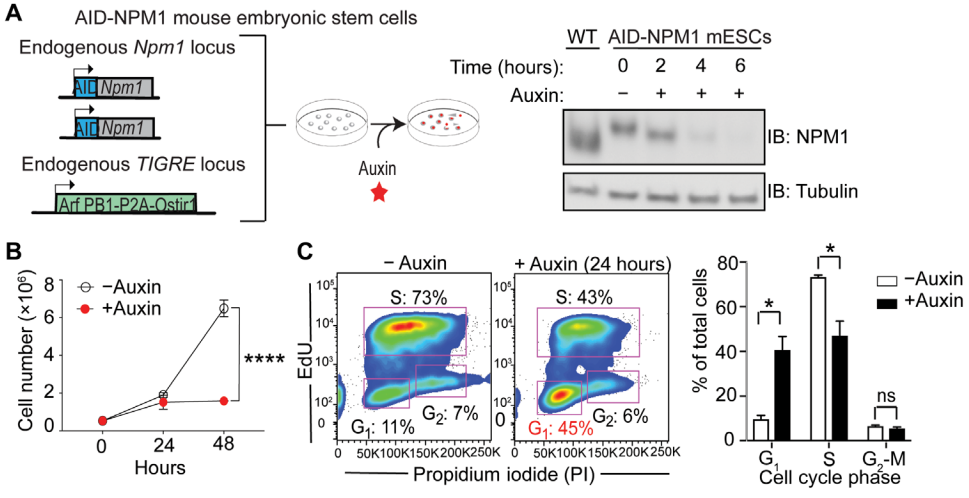

Fig. 2. Cell-cycle effects accompanying NPM1 depletion. (**A**) AID-NPM1 mESCs were generated using CRISPR knock-in such that an AID tag was appended to the 5′-end of the *Npm1* gene and the auxin-binding receptor, *Oryza sativa* TIR (Tir1), to the TIGRE locus (left). Western blot analysis of whole-cell extracts following the addition of auxin to AID-NPM1 mESCs in a time-dependent manner (0-, 2-, 4-, and 6-hour time points) showing that NPM1 is depleted within 6 hours (right). (**B**) Cell proliferation analysis of AID-NPM1 mESCs in the presence and absence of auxin over a 48-hour time period. Statistical significance was determined by two-way ANOVA (****$P < 0.0001$). (**C**) Cell-cycle analysis by flow cytometry of AID-NPM1 mESCs in G_1-, S-, and G_2-M phases based on the analysis of propidium iodide (DNA content) and EdU incorporation, in the presence and absence of auxin. The percentage of cells in each phase is shown on the right with significance determined by Student's *t* test (*$P < 0.05$). ns, not significant.

PRC2 target genes were more enriched in the up-regulated dataset (Fig. 3E), suggesting that NPM1 depletion alters gene repression. A Gene Ontology (GO) analysis indicated that the top five sets of derepressed genes were related to development (Fig. 3F). Of note, a naturally occurring, heterozygous mutated *NPM1* allele ($NPM1c^+$) exhibits abnormal cytoplasmic retention and is associated with ~35% of acute myelogenous leukemia (AML) with normal karyotype (*23*). Previous studies demonstrated that $NPM1c^+$ AML exhibits derepression of specific *HOXA* and *HOXB* loci (*24*). In accordance, the AID-NPM1 cells exhibited increased transcription at the *HoxA9*, *HoxB4*, and *Gata2* loci as a function of auxin treatment for 12 hours after S-phase release, as evidenced by RNA sequencing (RNA-seq) (Fig. 3G). Derepression of these PRC2 target genes was detectable early in late S phase (fig. S3), when AID-NPM1 was depleted (Fig. 3A). In contrast, expression of transcriptionally active *Pou5f1* and *Ccna2* genes was unaltered (fig. S3).

NPM1 depletion thwarts inheritance of H3K27me3-chromatin domains

To examine whether NPM1 fosters epigenetic inheritance and, in particular, through H3K27me3-modified nucleosomes, we revisited the CRISPR-Cas9 biotinylation system that captured the inheritance of biotinylated parental nucleosomes specifically from repressed loci during DNA replication at single-locus resolution (*1*) but now in the context of NPM1 depletion. We examined anew two such loci, *Gata2* and *Gata6*, whose expression is inducible and which lost parental nucleosome inheritance upon activation with retinoic acid (*1*). We rebuilt the CRISPR-Cas9 biotinylation system (Fig. 4A) in

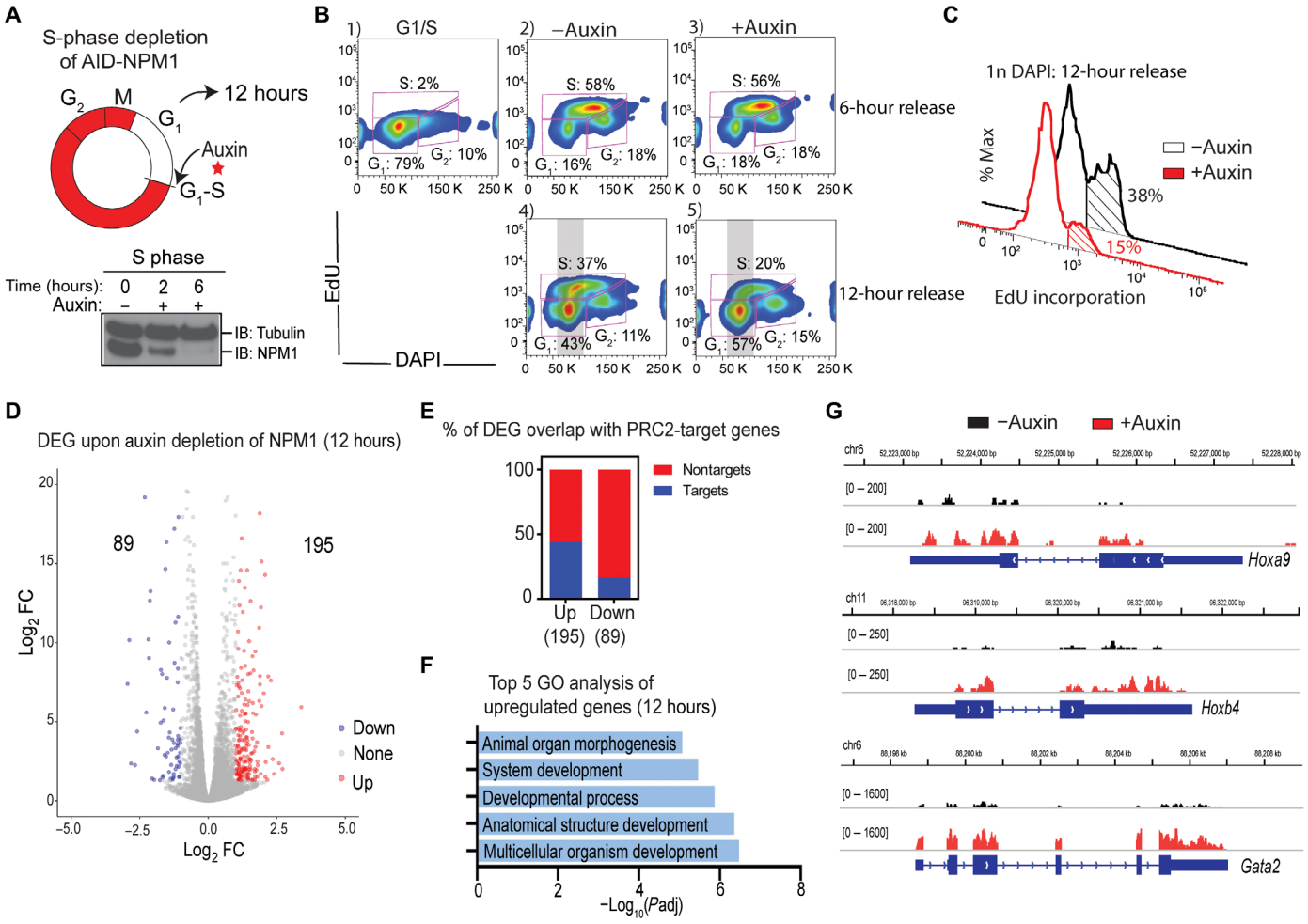

Fig. 3. Altered gene expression upon depletion of NPM1. (**A**) Schematic showing the protocol for S-phase specific addition of auxin to AID-NPM1 cells (top). Cells were synchronized at G_1-S with a double thymidine block, and auxin was added upon washing and releasing cells into S phase. Western blot analysis shows depletion of NPM1 within a 6-hour release into S phase (bottom). For further analysis as in (B), cells were also harvested within the next G_1 phase (12-hour release). (**B**) Cell-cycle analysis by flow cytometry of AID-NPM1 cells in the presence and absence of auxin during a 6- and 12-hour release from the G_1-S-block. G_1-, S-, and G_2-M phases were designated on the basis of 4′,6-diamidino-2-phenylindole (DAP1) analysis and EdU incorporation. (**C**) Analysis of EdU incorporation by AID-NPM1 cells upon a 12-hour release in the presence and absence of auxin, taken from the DAPI stain within the gray area indicated in (B). (**D**) Differentially expressed genes (DEGs) identified by RNA-seq analysis of AID-NPM1 cells upon a 12-hour release in the presence and absence of auxin (two replicates each). (**E**) Percentage of DEGs from (D) that overlaps with PRC2/H3K27me3 ChIP-seq targets in mESC. (**F**) The Gene Ontology (GO) term enrichment of those genes that were derepressed in the presence of auxin as identified in (D). (**G**) Genome-browser screenshots of RNA-seq at *Hoxa9*, *Hoxb4*, and *Gata2* loci depicting results as normalized coverage tracks upon a 12-hour treatment with (red) and without (black) auxin in AID-NPM1 mESCs. Data represent one replicate of two.

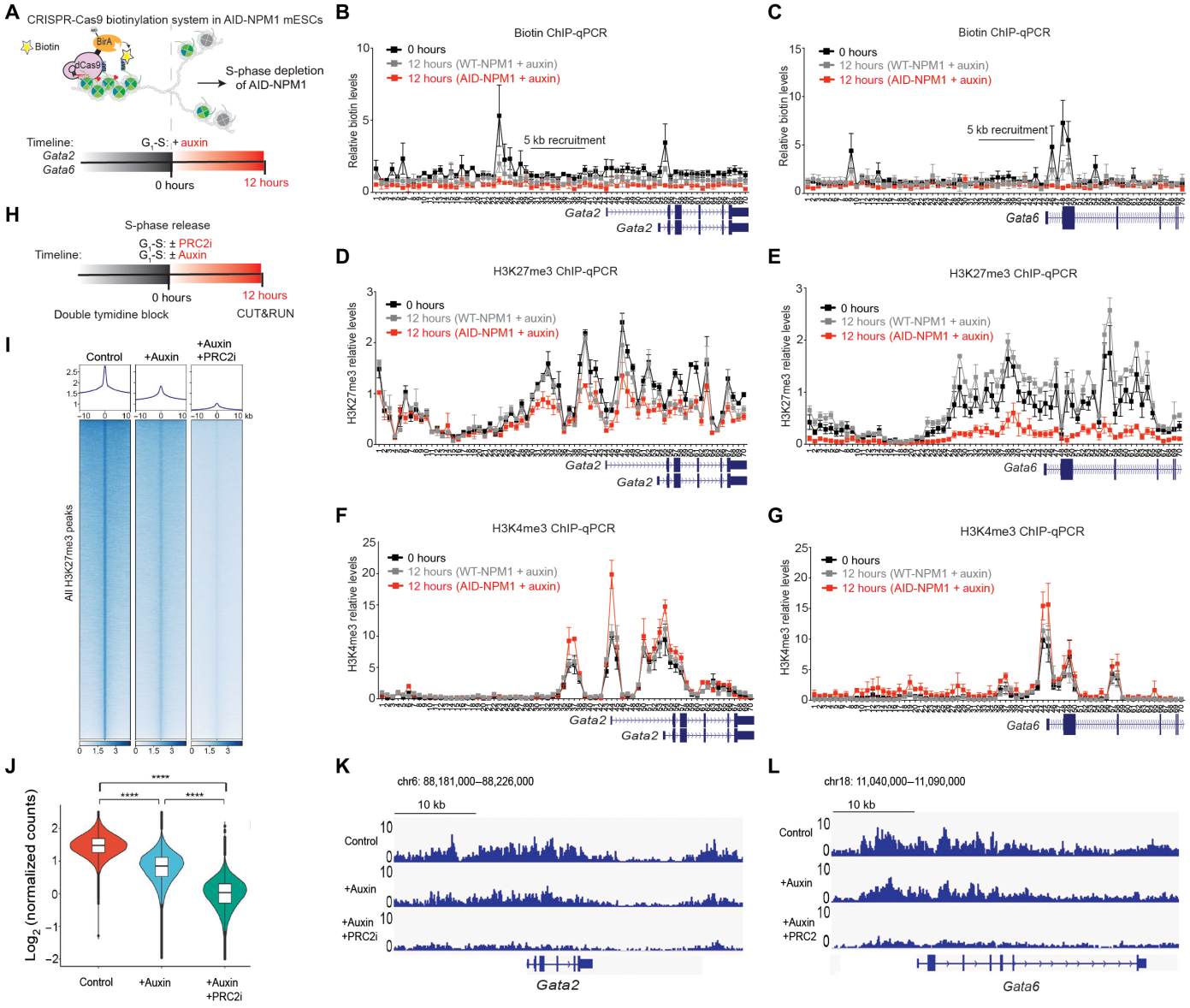

Fig. 4. Depletion of NPM1 thwarts inheritance of repressed chromatin domains. (**A**) Schematic of the previously reported CRISPR-Cas9 biotinylation system that captured the inheritance of repressed, but not active, chromatin domains during S phase, in this case using AID-NPM1 cells treated or untreated with auxin. As previously described (*1*), G_1-S–blocked AID-NPM1 or WT-NPM1 cells received a 6-hour pulse of Dox to induce expression of an engineered dCas9-BirA-AID fusion protein, exogenous biotin to mark nucleosomes, and gRNAs for targeting BirA to the *Gata2* or *Gata6* loci. Cells were then released into S phase for 12 hours as previously described, but now in the presence auxin. Cells were then processed for (**B** and **C**) native mononucleosomal biotin ChIP-qPCR for *Gata2* (B) or *Gata6* (C) loci, (**D** and **E**) H3K27me3 ChIP-qPCR for *Gata2* (D) or *Gata6* (E) loci, and (**F** and **G**) H3K4me3 ChIP-qPCR for *Gata2* (F) or *Gata6* (G) loci. The *x* axis represents primer pairs spanning mm10 Chr6:88,172,429-88,207,234 for *Gata2* and Chr18:11,030,846-11,065,352 for *Gata6*. (**H**) A depiction of the experimental flow for treatment with auxin as a function of the presence of the PRC2 inhibitor (GSK126), followed by CUT&RUN. (**I**) Heatmaps of H3K27me3 CUT&RUN using AID-NPM1 cells treated as in (H). Top, line plots of relative quantifications based on averaged intensities of all H3K27me3 peaks detected. Bottom, all H3K27me3 peaks centered by max peak intensity within a ±10 kb window. (**J**) Statistics and quantification of H3K27me3 CUT&RUN shown in (H). Violin plot of the $\log_2$(normalized counts) under the different conditions as indicated (****$P < 0.0001$). (**K** and **L**) Representative tracks of the *Gata2* (K) and *Gata6* (L) loci from the H3K27me3 CUT&RUN experiments described in (H) to (J).

the AID-NPM1 and wild-type (WT)–NPM1 cell line that expresses four FLAG-BAP–tagged H3.1 alleles. We stably expressed a doxycycline-inducible version of dCas9 that is fused to BirA that biotinylates BAP (dCas9-BirA), as used previously (*1*). In lieu of the FKBP degron used previously, dCas9-BirA was now fused to an AID tag (dCas9-BirA-AID) that similarly ensures its limited presence to the G_1 phase and its absence in the S phase. Using this system, we gauged parental nucleosome inheritance as a function of the presence of NPM1 using stably expressed guide RNAs (gRNAs) that specifically target dCas9-BirA-AID to the *Gata2* or *Gata6*.

G_1-S–arrested AID-NPM1 and WT-NPM1 control cells were treated with limited doxycycline to induce dCas9-BirA-AID expression and biotin to label the appropriate FLAG-BAP-H3.1 for 6 hours, as performed previously (*1*). The cells were then released into S phase for

12 hours as performed previously but, this time, as a function of the presence of auxin that targets dCas9-BirA-AID and AID-NPM1 or only dCas9-BirA-AID in the case of WT-NPM1 cells. Chromatin IP (ChIP)–quantitative polymerase chain reaction (qPCR) for biotin demonstrated that the parental nucleosome inheritance evident at both the *Gata2* and *Gata6* loci in the case of untreated cells was lost in the case of auxin-treated cells that were depleted of NPM1 (Fig. 4, B and C, respectively), strongly suggesting that NPM1 is required for parental nucleosome inheritance from repressed loci. While *Gata2* and *Gata6* expression levels were quite modestly elevated upon depletion of AID-NPM1 (fig. S3), these loci still comprised nucleosomes having the repressive histone modification, H3K27me3, albeit at lower levels (Fig. 4, D and E). Notably, these developmentally regulated genes are inherently bivalent, comprising both H3K27me3 and H3K4me3 (*25*–*28*). An increased presence of H3K4me3 was evident at both loci under these conditions (Fig. 4, F and G). Given that PRC2 associates with replicating DNA (*29*–*31*), we reasoned that the levels of H3K27me3 detectable in the absence of NPM1 might arise de novo from PRC2-mediated catalysis of H3K27me3 on naïve nucleosomes that were randomly deposited on repressed domains.

To examine the contribution of de novo H3K27me3 catalysis by PRC2 upon release from S phase, we treated the synchronized AID-NPM1 cells with auxin as a function of the presence of the PRC2 inhibitor (PRC2i), GSK126, which targets EZH2 (*32*) (Fig. 4H). We used a high dose of GSK126 (5 μM) to achieve an efficient and acute inhibition of PRC2. As expected, treatment with auxin resulted in a significant, ~50% reduction in global H3K27me3 compared to control cells (shown by line plots, heatmaps, and violin plots from H3K27me3 CUT&RUN experiments, Fig. 4, I and J). However, cells cotreated with auxin and PRC2i exhibited a considerably greater reduction in H3K27me3 deposition after exiting S phase (12 hours). This effect was apparent not only at the *Gata2* and *Gata6* loci (Fig. 4, K and L) but also genome-wide (Fig. 4, I and J), consistent with NPM1 being key to parental nucleosome redeposition at repressive loci.

NPM1 is a demonstrated chaperone in nucleosome assembly, with its central region containing two acidic patches/domains (AD2 and AD3) that bind to histones and are required for its chaperone activity (Fig. 1E) (*18*, *33*). We probed AD2, AD3, and AD2+3 compound mutants to ascertain whether these regions of NPM1 are involved in the inheritance of repressed chromatin domains. We performed rescue experiments by ectopically expressing HA-tagged versions of NPM1, either WT or mutant in the indicated acidic patch(es), in auxin-treated AID-NPM1 cells (fig. S4A). Biotin-labeling through dCas9-BirA-AID was targeted to the representative *Gata2* locus. Although the polyclonal NPM1 antibody does not detect the NPM1 mutants efficiently, the expression of ectopically expressed NPM1 candidates was comparable in all cases as confirmed by HA antibody (fig. S4A). Biotin-ChIP-qPCR indicated that while auxin-resistant, WT NPM1 rescued the deficiency of histone redeposition, each of the NPM1 chaperone mutants failed to rescue this inheritance (fig. S4B), suggesting that NPM1 chaperone activity may contribute to this feature of the epigenetic process.

DISCUSSION

That epigenetic information in the form of histone modifications is directly transmitted to cell progeny was recently demonstrated in the case of repressed, but not active, chromatin domains (*1*, *2*). The local recycling of parental nucleosomes within facultative heterochromatin domains fosters the appropriate gene expression profiles in daughter cells. Here, we identified NPM1 as an integral component of this process, functionally sustaining H3K27me3-chromatin domains across DNA replication. This inheritance provides PRC2 with the allosteric activator, H3K27me3, which fosters its feed-forward mechanism and, thus, the full restoration of repressed chromatin states across S phase. Given that we detected interaction between NPM1 and PRC2 and between NPM1 and MCM2, we speculate that NPM1 may coordinate an aspect of the DNA replication process with that of the full restoration of repressed chromatin domains, respectively. Future experiments entailing coimmunofluorescence will help monitor the nuclear colocalization of NPM1/PRC2/MCM2 in the context of DNA replication. Our results also support that in the absence of NPM1, PRC2 is capable of de novo H3K27me3 catalysis on randomly placed naive nucleosomes. Yet, the levels of H3K27me3 attained in the absence of NPM1 were suboptimal. The absence of NPM1 gave rise to the loss of the fully repressed status of the *Gata2* locus. Given its essentiality, the effect of the long-term loss of NPM1 is not a tenable study. Nonetheless, we speculate that such a loss would not only thwart the inheritance of nucleosomes comprising H3K27me3 but also deprive PRC2 of substrate for its allosteric activation, giving rise to rampant gene derepression. While our results suggest that the histone chaperone activity of NPM1 may contribute to the local inheritance of parental nucleosomes from repressed chromatin domains, we look forward to understanding the precise molecular mechanism(s) involved: whether NPM1 chaperone activity is directly involved and given specificity for repressed chromatin domains through NPM1 interaction with MCM2 and/or PRC2, as well as how the specific dynamics of these NPM1-targeted interactions foster this aspect of epigenetic inheritance.

MATERIALS AND METHODS

Cell line generation

KH2 mouse ESCs used in this study were grown in Dulbecco's modified Eagle's medium (DMEM) supplemented with 15% fetal bovine serum (FBS), L-glutamine, penicillin-streptomycin, nonessential amino acids, 0.1 mM β mercaptoethanol, leukemia inhibitory factor, and 2i inhibitors, which include 1 μM mitogen-activated protein kinase kinase 1/2 inhibitor (PD0325901) and 3 μM glycogen synthase kinase 3 inhibitor (CHIR99021) on 0.1% gelatin-coated plates. 293T cells were used for lentiviral production and grown in DMEM supplemented with 10% FBS, L-glutamine, and penicillin-streptomycin.

Targeting of mESCs to endogenously express H3.1 genes comprising FLAG-BAP at the N terminus was described previously [(*1*); cell line 30-55-15], with the genotype of the cells used in this study presented in fig. S1A. Briefly, gene editing of the *Hist1h3* locus to incorporate FLAG-BAP tags was done by using ~750 bp gBlock for each gene, ordered from IDT or Genscript. These gBlocks included (i) a homology arm corresponding to ~350 to 450 bp of the H3 promoter area, (ii) the FLAG-BAP sequence placed after the start codon (FLAG-BAP sequence: GACTACAAAGACGATGACGACAAGG-GCCTGACAAGAATCCTGGAAGCTCAGAAGATCGTGAGAG-GAGGCCTCGAG), and (iii) a homology arm corresponding to ~200 to 300 bp of the H3.1 coding sequence. The PAM sequences of the gBlocks were mutated for correct Cas9 digestion of genomic DNA within cells. ESCs were then transfected with 0.5 μg of Cas9-gRNA-BFP plasmid targeting the promoter of H3.1 genes and 0.5 μg of amplified gBlock in Lipofectamine 2000 (Invitrogen) containing 2i

media. Transfected cells were fluorescence-activated cell sorter (FACS)–sorted and seeded at 20,000 cells per 15-cm plate, and 7 to 10 days later, single ESC clones were selected and plated onto individual wells of a 96-well plate for genotyping. Genomic DNA was harvested via QuickExtract (Epicentre) DNA extraction, and genotyping PCRs were performed using primers surrounding the target site. The PCR products of the FLAG-BAP–positive clones were purified and sequenced to verify the presence and correct sequence of a FLAG-BAP-H3 insertion. Primers for gRNA, gBlocks, and genotyping are shown in table S3.

For targeting of *NPM1*, a gBlock of approximately of 1897 bp was ordered from Genscript, which included (i) a homology arm corresponding to ~850 bp of the *NPM1* promoter, (ii) the *IAA17* 71 to 113 mRNA sequence with a 3× Glycine linker placed after the start codon (AID-3×Gly sequence: CCTAAAGATCCAGCCAAACCTC-CGGCCAAGGCACAAGTTGTGGGATGGCCACCGGTGA-GATCATACCGGAAGAACGTGATGGTTTCCTGCCAAAAAT-CAAGCGGTGGCCCGGAGGCGGCGGCGTTCGTGGGTG-GAGGT), and (iii) a homology arm corresponding to ~900 bp of the *NPM1exon1* and *NPM1intron1*. The PAM sequence of the gBlock was mutated to correct Cas9 digestion of the genomic DNA within cells, and cells were transfected with 0.5 μg of the Cas9-*NPM1*gRNA–green fluorescent protein (GFP) plasmid, FACS-sorted, and genotyped as above (table S3 for gRNA, gBlocks, and genotyping primer sequence). To check for correct in-frame insertion of *IAA17* to the *NPM1* transcript, RNA was purified from homozygous *IAA17-NPM1* genotype mESCs followed by cDNA synthesis. The cDNA was then used to amplify the *IAA17-NPM1* full-length transcript with a Q5/Taq polymerase mix and subsequently cloned into the TOPO-TA vector. The *IAA17-NPM1* mRNA transcript in the TOPO vector was sequenced using the M13 primers. The mESC clones that showed the correct sequence were selected and whole cell extract was taken for Western blots to observe the relative increase in the molecular weight of AID-NPM1 protein. Last, to obtain an optimized auxin-induced degron system (*22*), these AID-NPM1 mESCs were targeted at the TIGRE locus to contain ubiquitous expression of the auxin-binding receptor, *Oryza sativa TIR* (OsTir1 or TIR) (*22*). TIGRE gRNAs and a GFP-ARF16-PB1-OsTIR gBlock were transfected into AID-NPM1 mESCs and screened for GFP integration and auxin inducibility of AID-NPM1 degradation in GFP^+ mESCs. For auxin-induced degradation of AID-NPM1, 2.5 mM auxin was added to the cultures for the time frames indicated in the figures.

To generate dCas9-BirA-AID expressing stable cell lines used for biotinylation experiments, 2 μg of pINTA-dCas9-BirA-AID plasmid was transfected with Lipofectamine 2000 into FLAG-BAP-H3.1; AID-NPM1; TIR KH2 ESCs. After 2 weeks of Zeocin (200 μg/ml) selection, single colonies were selected and dCas9-BirA-AID inducibility was tested with doxycycline. Cells were then transduced with gRNAs tiling the *Gata2* and *Gata6* locus, as described previously (*1*) for downstream biotinylation experiments. For proteomics studies, which required expression of HA-MCM2 in mESCs, HA-MCM2 was inserted into pLVX-EF1a-IRES-ZsGreen1 (see cloning below), and lentiviruses were made and transduced into FLAG-BAP-H3.1 KH2 mESCs. Lentivirus production in 293T cells and transduction of KH2 mESCs was previously described (*1*).

Cell-cycle synchronization and analysis

For G_1 synchronization experiments, mESCs were plated at 50 to 60% confluency and pulsed for 18 hours with 8 μM thymidine, followed by a phosphate-buffered saline (PBS) wash and a 7- to 8-hour release into 2i media. mESCs were then given a second thymidine treatment at a 5 to 6 μM concentration for 12 to 13 hours. The G_1 block was confirmed by staining DNA with propidium iodide. For cell-cycle analysis using EdU labeling, Invitrogen's Click-iT EdU Cell Proliferation Kit for Imaging 488/564 dye was used. The biotinylation experiments were performed as described previously (*1*); however, for auxin depletion of NPM1 in S phase, cells were given 2.5 mM auxin immediately after releasing cells from a G_1-S block after the second thymidine treatment.

Cloning

To generate pLVX-EF1a-IRES-ZsGreen1-HA-MCM2, mouse MCM2 cDNA (Horizon discovery-Dharmacon) was amplified with Q5 polymerase using primers containing an HA tag followed by a 5×Gly linker synthesized by IDT (see table S4). PCR product and pLVX-EF1a-IRES-ZsGreen1 vector were digested with Xba I and Bam HI, ligated, and transformed into XL10 Gold competent cells. Colonies were picked and correct cloning was confirmed by sequencing. To generate constructs pFastbac1-6× His-FLAG-TEV-NPM1 and pFastbac1-6× His-FLAG-TEV-MCM2 and to purify NPM1 and MCM2 protein from SF9 cells, primers were synthesized from IDT containing 6× His- and FLAG-tag followed by the TEV recognition site (6× His-FLAG-TEV-) with the start of either the NPM1 or MCM2 coding sequence (see table S4). Primers were used to amplify mouse NPM1 (Horizon discovery-Dharmacon) and MCM2, and the product was digested with Bam HI and Eco RI and ligated with digested pFastbac1 (Invitrogen). The ligated product was transformed into XL10 Gold competent cells, and colonies were picked and correct cloning was confirmed by Sanger DNA sequencing.

For subcloning of GFP-ARF16-PB1-P2A-OsTIR1 into a TIGRE donor plasmid, GFP-ARF16-PB1-P2A-OsTIR-SV40(PolyA) was amplified from pMGS56, a gift from M. Guertin (Addgene plasmid no. 129668; http://n2t.net/addgene:129668; RRID:Addgene_129668), and digested with Mlu I and Not I. The pEN396 TIGRE donor plasmid, a gift from B. Bruneau (Addgene plasmid no. 92142; http://n2t.net/addgene:92142; RRID:Addgene_92142), was digested with Mlu I and Not I and ligated to digested GFP-ARF16-PB1-P2A-OsTIR-SV40(PolyA). The ligated pEN396- GFP-ARF16-PB1-P2A-OsTIR-SV40(PolyA) was transformed into XL10 Gold competent cells and correct cloning was confirmed by Sanger DNA sequencing. The pX330-EN1201 (Cas9 + sgRNA against mouse TIGRE acceptor locus) was used along with pEN396-GFP-ARF16-PB1-P2A-OsTIR-SV40(PolyA) to make inducible AID-NPM1 KH2 mESCs, as described above.

For cloning of IAA17 (amino acids 71 to 113 of the AID protein) into pINTA-N3-dCas9-BirA previously described (*1*), Gibson cloning was performed. The ~250-bp gBlock containing BirA-linker(5×A-la-Gly)-AID-STOP (5′-CGACAAGCAGGGAGCTCTGCTGCTG-GAGCAGGACGGAATCATCAAGCCCTGGATGGGC-GGAGAAATCTCCCTGAGAAGCGCAGAGAAGGGAGCTG-GTGCAGGCGCTGGAGCGGGTGCCCCTAAAGATCCAGC-CAAACCTCCGGCCAAGGCACAAGTTGTGGGATGGCCAC-CGGTGAGATCATACCGGAAGAACGTGATGGTTTCCTGC-CAAAAATCAAGCGGTGGCCCGGAGGCGGCGGCGTTCGT-GTAG-3′) was Gibson-cloned into pINTA-N3-dCas9-BirA using primers described in table S4. Transformation of the Gibson reaction followed by Sanger DNA sequencing of clones provided confirmation of the correct fusion of dCas9-BirA-AID.

To generate pLVX-TRE3G-mCherry-HA-NPM1wt for rescue experiments as well as HA-stepwise deletion of NPM1AD1 and

NPM1AD2 mutants to generate compound mutant HA-NPM1AD1+AD2, the restriction enzymes Mlu I and Eco RI were used to clone into the pLVX-TRE3G-mCherry (Clontech). For the full-length amplification of NPM1, primers were synthesized from IDT with forward primer containing the Mlu I restriction site, Kozak sequence, the HA-tag sequence, and a 5× Glycine linker (table S4). Next, for each of the acidic mutants (HA-NPM1AD1, HA-NPM1AD2, and HA-NPM1AD1 + AD2), PCR fusion was conducted to delete 120 to 133 amino acids and/or 159 to 188 amino acids of NPM1 protein (table S4). PCR products were then digested with Mlu I and Eco RI followed by ligation and transformation into XL10 Gold competent cells. Colonies were picked and correct cloning was confirmed by Sanger DNA sequencing.

Protein purification using baculovirus expression system

The purification of PRC2 was described previously (*34*). To purify mouse 6× His-FLAG-TEV-NPM1 and 6× His-FLAG-TEV-MCM2, the proteins were expressed in Sf9 cells by baculovirus infection. After 60 hours of infection, Sf9 cells were resuspended in BC150 buffer [25 mM Hepes-NaOH (pH 7.8), 1 mM EDTA, 150 mM NaCl, 10% glycerol, 1 mM dithiothreitol (DTT), and 0.1% NP-40] with protease inhibitors [1 mM phenylmethlysulfonyl fluoride (PMSF), 0.1 mM benzamidine, leupeptin (1.25 mg/ml), and pepstatin A (0.625 mg/ml)] and phosphatase inhibitors (20 mM NaF and 1 mM Na_3VO_4). Cells were lysed by sonication (Fisher Sonic Dismembrator model 100), and NPM1 or MCM2 was tandemly purified through Ni–nitrilotriacetic acid (NTA) agarose beads (Qiagen) and FLAG-M2 agarose beads (Sigma-Aldrich), digested with His-TEV protease, and subjected to another purification with Ni-NTA agarose beads to remove any TEV contaminant as well as tagged full-length proteins (final product shown in fig. S1D).

Whole-cell extract and Western blotting

Cells were harvested and lysed with CHAPS-urea buffer [50 mM tris-HCl (pH 7.9), 8 M urea, and 1% CHAPS] containing protease inhibitors [0.2 mM PMSF, pepstatin A (1 μg/ml), leupeptin (1 μg/ml), and aprotinin (1 μg/ml)] and phosphatase inhibitors (10 mM NaF and 1 mM Na_3VO_4). The cell suspension was briefly sonicated (40% amplitude, five strokes) and centrifuged at 20,000*g* at 4°C for 20 min. The supernatant was collected, and protein concentrations were quantified via a bicinchonic acid assay. Proteins were separated using a 6 to 12% bis-tris SDS–polyacrylamide gel electrophoresis gel and transferred onto a polyvinylidene difluoride membrane. Membranes were blocked with 5% milk in phosphate-buffered saline tween (PBST) at room temperature for 1 hour and incubated with primary antibody overnight at 4°C. Membranes were washed three times with trish-buffered saline tween (TBST) and then incubated with horseradish peroxidase–conjugated secondary antibodies for 1 hour at room temperature, followed by exposure to enhanced chemiluminescence. Antibodies: NPM1 Abcam catalog no. ab15440, H3K27Me3 Cell Signaling catalog no. 9733, H3K27Me2 Cell Signaling catalog no. 9728, H3 Abcam catalog no. ab12079, H4 Abcam catalog no. ab10158, Tubulin Abcam catalog no. ab6046, Cas9 Millipore catalog no. MAC133-clone7A9, EED in-house, EZH2 in-house, SUZ12 Cell Signaling catalog no. 3737, H3K36me3 Abcam catalog no. ab9050, and H3K9me3 Abcam catalog no. ab8898.

In vivo biotinylation followed by native chromatin preparation

For in vivo biotinylation experiments using FLAG-BAP-H3.1; AID-NPM1 Kh2 mESCs, a similar protocol as described in (*1*) was followed. Briefly, mESCs were G_1-S–synchronized with double thymidine (as described above). mESCs were given a 6-hour pulse of doxycycline (2 μg/ml) and exogenous biotin (1 μg/ml) during the latter half of the second thymidine treatment (12 to 13 hours). Next, mESCs were either harvested at the G_1-G_2 block (starting time point, 0 hours) or washed with PBS and released to 2i media containing 2.5 mM auxin for the time points indicated. For acidic domain mutants in fig. S4, cDNA encoding HA-tagged NPM1, either WT or -AD2, -AD3, or -AD2+3 mutants were subcloned into the pLVX-EF1alpha-IRES-mCherry lentiviral vector and transduced to the AID-NPM1 cell lines for stable expression before cell-cycle synchronization and AID induction. For preparation of native MNase chromatin, cells were harvested using hypotonic lysis TMSD buffer [40 mM tris (pH 7.5), 5 mM $MgCl_2$, and 0.25 M sucrose with protease inhibitors], nuclei were then resuspended in NIB-250 [15 mM tris-HCl (pH 7.5), 60 mM KCl, 15 mM NaCl, 5 mM $MgCl_2$, 1 mM $CaCl_2$, and 250 mM sucrose with protease inhibitors] containing 0.3% NP-40, and the chromosome pellet was washed with NIB-250 buffer. After washes, the pellet was resuspended in MNase digestion buffer (10 mM Hepes, 50 mM NaCl, 5 mM $MgCl_2$, and 5 mM $CaCl_2$ with protease inhibitors) and treated with MNase (Sigma-Aldrich) until a DNA fragment size of 150 to 300 bp (1 to 2 nucleosomes) was attained. The MNase reaction was stopped by addition of EGTA and spun down, and the supernatant was placed in a fresh tube. The chromatin pellet was further processed by adding the same volume of BC500 [40 mM tris (pH 7.5), 5 mM $MgCl_2$, 500 mM NaCl and 5% glycerol, and protease inhibitors] with EGTA, incubated for 30 min while rotating at 4°C, and spun, and BC500 supernatant was pooled with an equal volume of MNase-treated supernatant to acquire the starting chromatin material for ChIPs.

Native ChIP-qPCR

The protocol for native H3K27me3 and biotin ChIPs was described previously (*1*). Briefly, MNase-treated chromatin as above was preblocked with Dynabeads protein G (Invitrogen) and spun down, and the IP was set up with 100 μg of precleared chromatin and 0.5 μg of *Drosophila* S2 chromatin (spike-in at a 1:100 concentration) in 10 μg of biotin antibody (Bethyl A150-109A), 4 μg of H3K27me3 (Cell Signaling C36B11), or 4 μg of H3K4me3 (Abcam ab8580), and 0.2 μg of H2AV (Active Motif catalog no. 39715) and incubated overnight with slow rotation at 4°C. IPs were then washed three times with 1 ml of BC300 buffer [40 mM tris (pH 7.5), 5 mM $MgCl_2$, 300 mM NaCl, and 5% glycerol with protease inhibitors], once with 1 ml of BC100 buffer [40 mM tris (pH 7.5), 5 mM $MgCl_2$, 100 NaCl, and 5% glycerol with protease inhibitors], and a quick wash with 1 ml of tris-edta (TE) + 50 mM NaCl. Beads were then resuspended in 125 μl of TE and 3 μl of 10% SDS (TES) and incubated at 65°C for 1 hour followed by digestion for 2 to 4 hours with 8 μg of proteinase K at 55°C while shaking. All samples were PCR column–purified, eluted in 50 μl, and diluted 1:4 with water for further qPCR studies.

For qPCR quantification, 5 μl of SYBR Green I Master mix (Roche), ROX reference dye, 1 μl of 5 μM primer pair, and 4 μl of diluted DNA were mixed for PCR amplification and detected by QuantStudio 5 real-time PCR systems instrument (Thermo Fisher Scientific). The data were then quantified and described in the corresponding figure legends. For *Drosophila* S2 chromatin, primers were FWD: TGGCTAGACTTTTGCGTCCT and REV: TACCAAAAGCCGTCCAAATC. For tiling of the *Gata2* and *Gata6* locus, qPCR primers were as previously listed in (*1*). Native biotin enrichment levels were normalized to 5% input followed by *Drosophila* chromatin

spike-in levels. For time course experiments, data were minus-Dox (-Dox) control–normalized, and error bars represent SD of three biological replicates. GraphPad Prism 7.0 was used for statistical analysis [two-way analysis of variance (ANOVA)]. A P value ≤0.05 was considered statistically significant; ***$P < 0.001$ and ****$P < 0.0001$.

ChIP and protein digestion

The rapid IP mass spectrometry of endogenous proteins protocol (*35*) was used to identify protein-nucleosome interactions. Briefly, FLAG-BAP-H3.1 KH2 mESCs expressing HA-MCM2 and KH2 mESCs (untagged controls) were cross-linked with 1% (v/v) formaldehyde for 4 min at room temperature and quenched with glycine, and chromatin was isolated with nuclear extraction buffer 1 (LB1), pelleted, and resuspended in LB2. Chromatin was pelleted and resuspended in LB3 and sheared to 200 to 600 bp using Bioruptor (Diagnode). Cleared chromatin lysate samples were subjected to tandem purification, as follows. First, H3.1 chromatin was immunoprecipitated. using anti-FLAG M2 affinity gel (Sigma-Aldrich) overnight at 4°C. H3.1-enriched protein complexes were eluted twice with BC100 containing FLAG peptide (Sigma-Aldrich) (first elution for 6 hours and second elution for 2 hours), followed by a second IP using antibodies against either H3K27me2/3 or HA (Abcam catalog no. ab9110) overnight. Dynabeads Protein G beads (Invitrogen) were then added the next day for 2 to 4 hours, and the ChIP samples were washed 10 times with 1 ml of radioimmunoprecipitation assay (RIPA) buffer. All buffers included protease and phosphatase inhibitors [0.2 mM PMSF, pepstatin A (1 μg/ml), leupeptin (1 μg/ml), and aprotinin (1 μg/ml)] and phosphatase inhibitors (10 mM NaF and 1 mM Na_3VO_4), as well as 5 mM sodium butyrate. After the last RIPA wash and before trypsin digestion, beads were washed with 100 mM ammonium bicarbonate. To digest proteins, beads were resuspended in 50 mM ammonium bicarbonate containing trypsin/Lys-C mix (20 ng/μl; Promega) followed by overnight incubation at 37°C with vigorous shaking. Reactions were then transferred to new tubes, acidified by mixing with 20% heptafluorobutyric acid added to 1% final concentration followed by 5-min incubation at room temperature and 5-min centrifugation at 16,000*g*. Peptides from clarified samples were desalted using Pierce C18 spin tips (Thermo Fisher Scientific) according to the manufacturer's instructions, dried under vacuum, and dissolved in 0.1% formic acid. Peptide concentrations were measured on Nanodrop One (Thermo Fisher Scientific) at 205 nm.

Liquid chromatography–mass spectrometry analysis

Peptides were analyzed on Orbitrap Lumos Fusion mass spectrometer coupled with Dionex Ultimate 3000 UHPLC (Thermo Fisher Scientific). Peptides (1 to 2 μg) were resolved on 50-cm-long EASY-Spray column (Thermo Fisher Scientific) at flow rate 0.2 μl/min over 90-min gradient 4 to 40% acetonitrile in 0.1% formic acid followed by a steep 5-min increase to 96% acetonitrile and a 5-min step elution with 96% acetonitrile. Data-dependent acquisition method was based on published protocol (*36*), except each cycle was set to last 2 s.

Mass spectrometry data analysis

Raw mass spectrometry data were processed with Proteome Discoverer 2.1.1.21 (Thermo Fisher Scientific) and/or MaxQuant 1.6.6.0 (*37*, *38*). Protein database supplied to programs consisted of mouse proteome (www.uniprot.org/proteomes/UP000000589) combined with a list of known protein contaminants (distributed with MaxQuant). Sequest HT search engine within Proteome Discoverer was run with default mass tolerance parameters. Variable modifications were methionine oxidation, cysteine carbamidomethylation, lysine and protein N-terminal acetylation, lysine and arginine methylation, and phosphorylation on serine, threonine, and tyrosine. MS1-based label-free quantitation was done using Precursor Ions Area Detector module in Proteome Discoverer. Individual peptide intensities were normalized to total peptide amount. Protein intensities were calculated using the Top N method that considered three top-most abundant peptides per protein (*39*). In MaxQuant, Andromeda search engine was run with default parameters for mass tolerance. Variable modifications were methionine oxidation, cysteine carbamidomethylation, and protein N terminus acetylation. To increase number of identified and quantitated peptides, match between runs option was enabled. For label-free quantitation, integrated intensity was used instead of maximum intensity. In further analyses, protein intensities were normalized to that of Protein G followed by subtracting intensity in untagged controls for each dataset. A list of acquired candidate polypeptides were considered for further analysis if the protein was enriched in late S phase relative to early S phase in all four independent H3.1 and H3K27me2/3 experiments (Fig. 1C) and the two independent H3.1 and HA-MCM2 proteome analyses.

Co-IP in late S-phase mESCs

The G_1-S block of mESCs was performed as discussed above and followed by a release into S phase for 6 hours to collect the late S-phase mESCs. Co-IP in nuclear extract from late S-phase mESCs was performed as described previously (*40*). Briefly, nuclei were extracted using HMSD buffer [20 mM Hepes (pH 7.5) at 4°C, 5 mM $MgCl_2$, 250 mM sucrose, 25 mM NaCl, and 1 mM DTT] supplemented with protease inhibitors. The resulting nuclei pellets were resuspended in BC420 high-salt buffer [20 mM tris-HCl (pH 7.9), 1.5 mM $MgCl_2$, 0.42 M NaCl, 0.5 mM DTT, and 0.2 mM EDTA] supplemented with protease inhibitors. Lysates were then pelleted at 20,000*g* for 15 min at 4°C, and the supernatants were subjected to dialysis in buffer D (20 mM Hepes, 150 mM NaCl, 1.5 mM $MgCl_2$, 0.2 mM EDTA, and 5% glycerol) overnight at 4°C. For IP, 1 to 2 mg of nuclear extract was incubated with ~3 to 5 μg of antibody. After incubation at 4°C for 2 hours, 30 μl of protein G beads was added and incubated at 4°C overnight. Beads were washed five times with buffer D (20 mM Hepes, 150 mM NaCl, 1.5 mM $MgCl_2$, 0.2 mM EDTA, and 5% glycerol) and boiled in 1× SDS loading buffer.

RNA purification, reverse transcription-qPCR, and RNA-seq

Total RNA extractions were performed using the Roche High pure RNA isolation kit. Superscript III reverse transcription reagents (Invitrogen) and random hexamers were used to prepare cDNAs. For qPCR quantification, 5 μl of SYBR Green I Master mix (Roche), ROX reference dye, 1 μl of IDT PrimeTime Primer set for corresponding assays, and 1 μl of cDNA were mixed for PCR amplification and detected by QuantStudio 5 real-time PCR systems instrument. For quantitative analysis, *Hoxa9*, *Hoxb4*, *Hoxb13*, *Gata2*, *Gata6*, *Pou5f1*, and *Ccna2* expression was normalized to *Actb* expression. Primers were ordered from Primetime IDT. For RNA-seq, the first strand was synthesized using reverse transcription via Superscript III and random hexamers. The second strand was synthesized with deoxyuridine triphosphate to generate strand asymmetry using DNA polymerase I (NEB, M0209L) and the *Escherichia coli* ligase (Enzymatics, L6090L). RNA-seq libraries were constructed using

the protocol described in (*1*), quantified by Qubit double-stranded DNA HS Assay Kit quality, and checked by High Sensitivity D1000 ScreenTape. Libraries were then sequenced as 50-bp single-end reads on a NovaSeq 6000 platform.

RNA-seq analysis

Reads were aligned to the mouse reference genome mm10 using STAR with the following parameters: --outFilterMismatchNoverLmax 0.2 --outFilterMultimapNmax 1 --outSAMstrandField intronMotif --outSAMmapqUnique 60 --twopassMode Basic --outSJfilterReads Unique --outFilterIntronMotifs RemoveNoncanonical. Gene counts were calculated using featureCounts with the following parameters: -p -s 2 -t exon and RefSeq mm10 annotation downloaded from GENCODE.

The output gene count tables were used as input into DeSeq2 for normalization and differential expression analysis. Bigwig files were generated using deeptools and default parameters for visualization in integrative genomics viewer (IGV).

ChIP-seq data analysis

Reads were aligned to the mouse reference genome mm10 and dm6 for spike-in samples using Bowtie2 with default parameters. Reads of quality score less than 30 were removed using samtools, and PCR duplicates were marked using picard. Regions in mm10 genome blacklist were removed using bedtools, and bigwig files were generated using deeptools and the following parameters: --binSize 50 --normalizeUsing RPKM --ignoreDuplicates --ignoreForNormalization chrX --extendReads 250 for visualization in IGV. Peaks were called using MACS2 with the following parameters: -f BAM -g mm --keep-dup all --broad --broad-cutoff 0.1. Genomic peak annotation was performed with the R package ChIPseeker considering the region ±3 kb around the transcriptional start site (TSS) as the promoter. Peak overlapping analysis was performed using the Python package Intervene and visualized using the Python package Matplotlib.

For visualization of ChIP sequencing (ChIP-seq), uniquely aligned reads mapping to the mouse genome were normalized using dm6 spike-in as described previously (*41*). Heatmaps were performed using the functions computeMatrix followed by plotHeatmap and plotProfile from deepTools.

CUT&RUN library preparation and data analysis

The CUT&RUN experiments were performed using the CUTANA CUT&RUN assay (EpiCypher) following the manufacturer's instructions. Briefly, the nuclei of cells were isolated using the TMSD buffer as previously described (*42*). The nuclei were bound by activated concanavalin A beads, followed by nuclear membrane permeabilization, incubation of primary antibody overnight, and binding of antibody to pA-MNase fusion protein. The MNase was activated by CaCl at 4°C for 1 hour, and then stop buffer with *E. coli* spike-in DNA was added to stop the reaction. The DNA released into the supernatant was purified and subjected to library preparation and next-generation sequencing (NovaSeq 6000, Illumina) to a depth between 26M and 35M reads. Data were analyzed using the same pipeline and normalized using *E. coli* spike-in as described above for ChIP-seq. Violin plots were prepared using the multiBigwigSummary function from deeptools in BED-file, and using a bed file, the regions corresponding to H3K27me3 peak regions were identified under control conditions. *P* values in violin plots were calculated using nonparametric Wilcoxon test from the ggpubr R package where **** denotes $P < 0.0001$.

SUPPLEMENTARY MATERIALS

Supplementary material for this article is available at https://science.org/doi/10.1126/sciadv.abm3945

View/request a protocol for this paper from *Bio-protocol*.

REFERENCES AND NOTES

1. T. M. Escobar, O. Oksuz, R. Saldaña-Meyer, N. Descostes, R. Bonasio, D. Reinberg, Active and repressed chromatin domains exhibit distinct nucleosome segregation during DNA replication. *Cell* **179**, 953–963.e11 (2019).
2. G. Schlissel, J. Rine, The nucleosome core particle remembers its position through DNA replication and RNA transcription. *Proc. Natl. Acad. Sci. U.S.A.* **116**, 20605–20611 (2019).
3. T. M. Escobar, A. Loyola, D. Reinberg, Parental nucleosome segregation and the inheritance of cellular identity. *Nat. Rev. Genet.* **22**, 379–392 (2021).
4. R. Margueron, D. Reinberg, The Polycomb complex PRC2 and its mark in life. *Nature* **469**, 343–349 (2011).
5. J. A. Simon, R. E. Kingston, Occupying chromatin: Polycomb mechanisms for getting to genomic targets, stopping transcriptional traffic, and staying put. *Mol. Cell* **49**, 808–824 (2013).
6. L. Di Croce, K. Helin, Transcriptional regulation by Polycomb group proteins. *Nat. Struct. Mol. Biol.* **20**, 1147–1155 (2013).
7. S. Aranda, G. Mas, L. Di Croce, Regulation of gene transcription by Polycomb proteins. *Sci. Adv.* **1**, e1500737 (2015).
8. J. R. Yu, C. H. Lee, O. Oksuz, J. M. Stafford, D. Reinberg, PRC2 is high maintenance. *Genes Dev.* **33**, 903–935 (2019).
9. R. Margueron, N. Justin, K. Ohno, M. L. Sharpe, J. Son, W. J. Drury III, P. Voigt, S. R. Martin, W. R. Taylor, V. de Marco, V. Pirrotta, D. Reinberg, S. J. Gamblin, Role of the polycomb protein EED in the propagation of repressive histone marks. *Nature* **461**, 762–767 (2009).
10. O. Oksuz, V. Narendra, C.-H. Lee, N. Descostes, G. L. Roy, R. Raviram, L. Blumenberg, K. Karch, P. P. Rocha, B. A. Garcia, J. A. Skok, D. Reinberg, Capturing the onset of prc2-mediated repressive domain formation. *Mol. Cell* **70**, 1149–1162.e5 (2018).
11. N. Rhind, D. M. Gilbert, DNA replication timing. *Cold Spring Harb. Perspect. Biol.* **5**, a010132 (2013).
12. A. Groth, A. Corpet, A. J. L. Cook, D. Roche, J. Bartek, J. Lukas, G.`. Almouzni, Regulation of replication fork progression through histone supply and demand. *Science* **318**, 1928–1931 (2007).
13. N. Richet, D. Liu, P. Legrand, C. Velours, A. Corpet, A. Gaubert, M. Bakail, G. Moal-Raisin, R. Guerois, C. Compper, A. Besle, B. Guichard, G. Almouzni, F. Ochsenbein, Structural insight into how the human helicase subunit MCM2 may act as a histone chaperone together with ASF1 at the replication fork. *Nucleic Acids Res.* **43**, 1905–1917 (2015).
14. R. Foti, S. Gnan, D. Cornacchia, V. Dileep, A. Bulut-Karslioglu, S. Diehl, A. Buness, F. A. Klein, W. Huber, E. Johnstone, R. Loos, P. Bertone, D. M. Gilbert, T. Manke, T. Jenuwein, S. C. B. Buonomo, Nuclear architecture organized by Rif1 underpins the replication-timing program. *Mol. Cell* **61**, 260–273 (2016).
15. M. S. Lindstrom, NPM1/B23: A multifunctional chaperone in ribosome biogenesis and chromatin remodeling. *Biochem. Res. Int.* **2011**, 1–16 (2011).
16. J. K. Box, N. Paquet, M. N. Adams, D. Boucher, E. Bolderson, K. J. O'Byrne, D. J. Richard, Nucleophosmin: From structure and function to disease development. *BMC Mol. Biol.* **17**, 19 (2016).
17. L. J. Frehlick, J. M. Eirin-Lopez, J. Ausio, New insights into the nucleophosmin/nucleoplasmin family of nuclear chaperones. *Bioessays* **29**, 49–59 (2007).
18. M. Okuwaki, K. Matsumoto, M. Tsujimoto, K. Nagata, Function of nucleophosmin/B23, a nucleolar acidic protein, as a histone chaperone. *FEBS Lett.* **506**, 272–276 (2001).
19. M. Okuwaki, A. Iwamatsu, M. Tsujimoto, K. Nagata, Identification of nucleophosmin/B23, an acidic nucleolar protein, as a stimulatory factor for in vitro replication of adenovirus DNA complexed with viral basic core proteins. *J. Mol. Biol.* **311**, 41–55 (2001).
20. S. Grisendi, R. Bernardi, M. Rossi, K. Cheng, L. Khandker, K. Manova, P. P. Pandolfi, Role of nucleophosmin in embryonic development and tumorigenesis. *Nature* **437**, 147–153 (2005).
21. K. Nishimura, T. Fukagawa, H. Takisawa, T. Kakimoto, M. Kanemaki, An auxin-based degron system for the rapid depletion of proteins in nonplant cells. *Nat. Methods* **6**, 917–922 (2009).
22. K. M. Sathyan, B. D. McKenna, W. D. Anderson, F. M. Duarte, L. Core, M. J. Guertin, An improved auxin-inducible degron system preserves native protein levels and enables rapid and specific protein depletion. *Genes Dev.* **33**, 1441–1455 (2019).
23. B. Falini, C. Mecucci, E. Tiacci, M. Alcalay, R. Rosati, L. Pasqualucci, R. la Starza, D. Diverio, E. Colombo, A. Santucci, B. Bigerna, R. Pacini, A. Pucciarini, A. Liso, M. Vignetti, P. Fazi, N. Meani, V. Pettirossi, G. Saglio, F. Mandelli, F. Lo-Coco, P. G. Pelicci, M. F. Martelli, Cytoplasmic nucleophosmin in acute myelogenous leukemia with a normal karyotype. *N. Engl. J. Med.* **352**, 254–266 (2005).
24. L. Brunetti, M. C. Gundry, D. Sorcini, A. G. Guzman, Y.-H. Huang, R. Ramabadran, I. Gionfriddo, F. Mezzasoma, F. Milano, B. Nabet, D. L. Buckley, S. M. Kornblau, C. Y. Lin,

P. Sportoletti, M. P. Martelli, B. Falini, M. A. Goodell, Mutant NPM1 maintains the leukemic state through HOX expression. *Cancer Cell* **34**, 499–512.e9 (2018).
25. V. Azuara, P. Perry, S. Sauer, M. Spivakov, H. F. Jørgensen, R. M. John, M. Gouti, M. Casanova, G. Warnes, M. Merkenschlager, A. G. Fisher, Chromatin signatures of pluripotent cell lines. *Nat. Cell Biol.* **8**, 532–538 (2006).
26. B. E. Bernstein, T. S. Mikkelsen, X. Xie, M. Kamal, D. J. Huebert, J. Cuff, B. Fry, A. Meissner, M. Wernig, K. Plath, R. Jaenisch, A. Wagschal, R. Feil, S. L. Schreiber, E. S. Lander, A bivalent chromatin structure marks key developmental genes in embryonic stem cells. *Cell* **125**, 315–326 (2006).
27. T. S. Mikkelsen, M. Ku, D. B. Jaffe, B. Issac, E. Lieberman, G. Giannoukos, P. Alvarez, W. Brockman, T. K. Kim, R. P. Koche, W. Lee, E. Mendenhall, A. O'Donovan, A. Presser, C. Russ, X. Xie, A. Meissner, M. Wernig, R. Jaenisch, C. Nusbaum, E. S. Lander, B. E. Bernstein, Genome-wide maps of chromatin state in pluripotent and lineage-committed cells. *Nature* **448**, 553–560 (2007).
28. P. Voigt, G. LeRoy, W. J. Drury III, B. M. Zee, J. Son, D. B. Beck, N. L. Young, B. A. Garcia, D. Reinberg, Asymmetrically modified nucleosomes. *Cell* **151**, 181–193 (2012).
29. K. H. Hansen, A. P. Bracken, D. Pasini, N. Dietrich, S. S. Gehani, A. Monrad, J. Rappsilber, M. Lerdrup, K. Helin, A model for transmission of the H3K27me3 epigenetic mark. *Nat. Cell Biol.* **10**, 1291–1300 (2008).
30. C. Alabert, J. C. Bukowski-Wills, S. B. Lee, G. Kustatscher, K. Nakamura, F. de Lima Alves, P. Menard, J. Mejlvang, J. Rappsilber, A. Groth, Nascent chromatin capture proteomics determines chromatin dynamics during DNA replication and identifies unknown fork components. *Nat. Cell Biol.* **16**, 281–291 (2014).
31. A. Hugues, C. S. Jacobs, F. Roudier, Mitotic inheritance of PRC2-mediated silencing: Mechanistic insights and developmental perspectives. *Front. Plant Sci.* **11**, 262 (2020).
32. M. T. McCabe, H. M. Ott, G. Ganji, S. Korenchuk, C. Thompson, G. S. van Aller, Y. Liu, A. P. Graves, A. D. P. III, E. Diaz, L. V. LaFrance, M. Mellinger, C. Duquenne, X. Tian, R. G. Kruger, C. F. McHugh, M. Brandt, W. H. Miller, D. Dhanak, S. K. Verma, P. J. Tummino, C. L. Creasy, EZH2 inhibition as a therapeutic strategy for lymphoma with EZH2-activating mutations. *Nature* **492**, 108–112 (2012).
33. M. Okuwaki, The structure and functions of NPM1/Nucleophsmin/B23, a multifunctional nucleolar acidic protein. *J. Biochem.* **143**, 441–448 (2008).
34. C.-H. Lee, J.-R. Yu, S. Kumar, Y. Jin, G. L. Roy, N. Bhanu, S. Kaneko, B. A. Garcia, A. D. Hamilton, D. Reinberg, Allosteric activation dictates PRC2 activity independent of its recruitment to chromatin. *Mol. Cell* **70**, 422–434.e6 (2018).
35. H. Mohammed, C. Taylor, G. D. Brown, E. K. Papachristou, J. S. Carroll, C. S. D'Santos, Rapid immunoprecipitation mass spectrometry of endogenous proteins (RIME) for analysis of chromatin complexes. *Nat. Protoc.* **11**, 316–326 (2016).
36. S. Davis, P. D. Charles, L. He, P. Mowlds, B. M. Kessler, R. Fischer, Expanding proteome coverage with charge ordered parallel ion aNalysis (CHOPIN) combined with broad specificity proteolysis. *J. Proteome Res.* **16**, 1288–1299 (2017).
37. J. Cox, M. Mann, MaxQuant enables high peptide identification rates, individualized p.p.b.-range mass accuracies and proteome-wide protein quantification. *Nat. Biotechnol.* **26**, 1367–1372 (2008).
38. S. Tyanova, T. Temu, J. Cox, The MaxQuant computational platform for mass spectrometry-based shotgun proteomics. *Nat. Protoc.* **11**, 2301–2319 (2016).
39. J. C. Silva, M. V. Gorenstein, G. Z. Li, J. P. Vissers, S. J. Geromanos, Absolute quantification of proteins by LCMSE: A virtue of parallel MS acquisition. *Mol. Cell. Proteomics* **5**, 144–156 (2006).
40. S. Liu, K. A. Aldinger, C. V. Cheng, T. Kiyama, M. Dave, H. K. McNamara, W. Zhao, J. M. Stafford, N. Descostes, P. Lee, S. G. Caraffi, I. Ivanovski, E. Errichiello, C. Zweier, O. Zuffardi, M. Schneider, A. S. Papavasiliou, M. S. Perry, J. Humberson, M. T. Cho, A. Weber, A. Swale, T. C. Badea, C. A. Mao, L. Garavelli, W. B. Dobyns, D. Reinberg, NRF1 association with AUTS2-Polycomb mediates specific gene activation in the brain. *Mol. Cell* **81**, 4757 (2021).
41. D. A. Orlando, M. W. Chen, V. E. Brown, S. Solanki, Y. J. Choi, E. R. Olson, C. C. Fritz, J. E. Bradner, M. G. Guenther, Quantitative ChIP-Seq normalization reveals global modulation of the epigenome. *Cell Rep.* **9**, 1163–1170 (2014).
42. N. D. Fogarty, K. L. Marhaver, Coral spawning, unsynchronized. *Science* **365**, 987–988 (2019).

Acknowledgments: We are grateful to L. Vales for active discussions and help in writing the paper, to A. Loyola for active discussions, and to D. Hernandez for impeccable technical assistance. **Funding:** T.M.E. was supported by a 3R01CA199652-14S1 grant, J.-R.Y. was supported by the American Cancer Society (PF-17-035-01), and S.L. was supported by the Howard Hughes Medical Institute. All studies were supported by a grant from the NCI (9R-1CA199652-13A1) and by HHMI. **Author contributions:** T.M.E. directed some of the experiments, performed most of the experiments, and wrote most of the figure legends and Materials and Methods. J.-R.Y. performed and analyzed experiments described in Fig. 4 (J and K) and fig. S2, and wrote accompanying legends. S.L. performed bioinformatic analysis and helped with the interpretation of sequencing results. K.L. helped with the synchronizations of the mESCs and characterization of the AID-NPM1 mESC line. N.V. performed liquid chromatography–mass spectrometry and normalization of the raw data. E.N. oversaw mass spectrometry experiments. D.R. directed the experiments and oversaw the manuscript. **Competing interests:** D.R. is a cofounder of Constellation Biotechnology and Fulcrum. The authors declare that they have no other competing interests. **Data and materials availability:** The accession numbers for the raw data FASTQ files and processed files for all sequencing data are deposited in NCBI GEO (accession number: GSE183090). Requests for the plasmids and modified KH2 mES cell lines should be submitted to D.R. All data needed to evaluate the conclusions in the paper are present in the paper and/or the Supplementary Materials.

Submitted 14 September 2021
Accepted 9 March 2022
Published 27 April 2022
10.1126/sciadv.abm3945